

BMW Airhead Oil Filter Canister Displacement: Service Practice, Load Paths, and the \$2,000 O-Ring Myth

Custom Konrad

January 11, 2026

Abstract

The BMW Airhead oil filter canister sealing system is well known for its sensitivity to assembly tolerances and service configuration. This paper documents a latent failure mode in which a configuration that was locally compliant with parts documentation nevertheless produced an external oil leak through unintended geometric interaction.

Following a prolonged rebuild, oil leakage developed at the oil filter cover despite nominal O-ring installation and normal engine operation. Initial diagnosis focused on familiar elastomer preload and creep mechanisms. Subsequent inspection, however, revealed inward displacement of the thin-wall oil filter canister mouth caused by eccentric contact with an overlong oil pan fastener located directly beneath the sealing region.

A force-scale analysis demonstrates that once axial backing at the canister mouth is locally compromised, normal O-ring preload is sufficient to plastically deform thin stainless shims and drive seal extrusion, without requiring global overload, loss of retention, or excessive oil pressure. Geometric analysis shows how small radial disturbances at the mouth can induce rigid-body motion about a distal press-fit region, while retention behavior explains why the failure remains latent until leakage occurs.

The resulting failure mode is subtle, mechanically plausible, and easily misdiagnosed. More broadly, it illustrates a limitation of documentation-based safeguards: parts fiches ensure compatibility, but do not encode three-dimensional interference constraints in evolving service configurations. The lessons presented here generalize to other systems combining thin-walled features, tight sealing tolerances, and incremental hardware modifications.

1 Primary References and How to Reproduce Key Findings

Three complementary sources anchor this work, spanning parts identification, formal technical analysis, and practical service procedure. These references are cited throughout where applicable.

- **MaxBMW parts fiche (navigation path).** Navigate to [MaxBMW Fiche: DiagramsMain.aspx](#), select 11 -- Engine, and open Diagram #11_1688. In this diagram, the oil filter canister is identified as item 13. While the associated part number (11 11 1 338 203) is correct, the description is incorrectly listed as “STEERING COLUMN TUBE.” This mislabeling can cause confusion when relying solely on fiche-based identification, but was readily resolved through consultation with an experienced supplier such as **Max BMW Motorcycles**.
- **Largiader technical note on canisters and shimming.** See [largiader.com/tech/filters/canister.html](#). This reference provides a detailed discussion of early versus later canister designs, O-ring and shim stack geometry, and depth-control practices, including quantitative guidance and tabulated recommendations.
- **Brooks & Brandon, *Airhead Garage* (procedural reference).** See the YouTube video “[BMW Airhead Oil Filter \\$2000 O-Ring Explained](#)”. This source presents an experience-driven visual walk-through of oil filter and canister service, illustrating correct assembly order, common failure modes, and the practical consequences of tolerance mismanagement.

2 Background and Modification Context

The BMW Airhead oil filter system relies on a thin-wall steel canister installed into a deep cylindrical bore in the aluminum crankcase. Proper sealing is achieved by axial compression of a large elastomer O-ring at the canister mouth, optionally supplemented by one or more shims. The system is highly sensitive to canister depth (i.e., the distance from the crankcase face to the canister mouth), with acceptable variation on the order of tenths of a millimeter (see Largiader). Any axial displacement of the canister directly affects O-ring preload and seal integrity.

One of the oil pan fasteners is located immediately beneath the oil filter canister mouth. By design, this fastener is intentionally short in *all* configurations—whether a stock oil pan is installed or a distance ring and skid plate assembly is fitted—to prevent intrusion into the filter cavity and contact with the canister.

3 Observed Symptoms

Following completion of the rebuild—including installation of a Silent Hektik ignition (Z2070 Microlino), three-phase regulator/rectifier (R1335eco), and alternator (V1335 LiMa)—the engine was started after a prolonged period of non-operation. The engine started immediately and ran smoothly, with nominal ignition timing, charging behavior, and idle quality. However, oil leakage developed at the oil filter cover shortly after startup as crankcase pressure increased.

Given the extended downtime and the well-known sensitivity of the Airhead oil filter sealing system, the initial diagnosis focused on loss of O-ring preload or elastomer creep, consistent with the familiar “\$2,000 O-ring” failure narrative.

4 Root Cause Discovery

The O-ring visible in Fig. 1 appears nominal and is included primarily for reference. Its mechanical role is indirect but decisive: once local support at the canister mouth was compromised, the O-ring—effectively incompressible in volume—continued to transmit its axial preload into the seal stack. With the load path constrained by the surrounding geometry, this preload was redistributed into the unsupported portion of the shim, producing smooth local plastic bending without requiring global overload or gross misalignment. In this condition, the O-ring transitions from a compliant sealing element to an effective load-transmitting medium.

To place the observed deformation behavior on a physically meaningful footing, the following analysis is presented as a *force-scale sanity check*, not as a seal design calculation.

Order-of-magnitude estimate of localized O-ring load transmission. Using standard O-ring compression-load data for a 70A elastomer, a circular O-ring with 4 mm cross-section subjected to 10–25% squeeze typically develops a compressive line load on the order

of $f \approx 20\text{--}90$ lbf/in of circumference at room temperature.¹ For the present geometry, with center diameter $D_c = 50$ mm and circumference $L = \pi D_c = 157$ mm = 6.19 in, this corresponds to a total stored compressive force of

$$F_{\text{total}} = fL \approx 0.55\text{--}2.5 \text{ kN}.$$

If uniform backing is lost and the O-ring load is instead transmitted through only a fraction α of the circumference, the effective local line load increases approximately as $f_{\text{local}} \approx f/\alpha$. For a plausible localization $\alpha = 0.10\text{--}0.25$ and an estimated contact patch width $w \sim 1$ mm, the implied local contact pressure scales as

$$p_{\text{local}} \approx \frac{f_{\text{local}}}{w},$$

yielding pressures in the tens of megapascals even before accounting for further geometric concentration. Although operation at 100°C reduces the effective modulus of the elastomer, the qualitative conclusion remains unchanged: loss of backing strongly amplifies local stress transmission.

The susceptibility of the stainless shims to plastic deformation can be assessed by modeling a $t = 0.3$ mm shim as a thin strip spanning a locally unsupported region of width ℓ . For a simply supported strip under uniform pressure p , the maximum bending stress is

$$\sigma_{\text{max}} \approx \frac{3p\ell^2}{4t^2},$$

from which the pressure required to reach yield may be estimated as

$$p_y \approx \frac{4\sigma_y t^2}{3\ell^2}.$$

Taking a representative stainless yield strength of $\sigma_y \approx 200$ MPa gives $p_y \approx 24$ MPa for $\ell = 1$ mm and $p_y \approx 6$ MPa for $\ell = 2$ mm. These values fall well within the range of localized pressures implied above, demonstrating that once uniform backing is compromised, even modest nominal O-ring squeeze can generate sufficient localized stress to plastically dish or dent thin metallic shims. In this regime, the O-ring no longer acts solely as a compliant sealing element, but functions as an effective load-transmitting medium.

¹Values are consistent with published compression-force guidance for 70A elastomers; elevated temperature effects are addressed below.

Comparison to oil-pressure-induced separation force. The force transmission capacity implied by the O-ring preload can be placed in context by comparing it to the hydraulic force generated by normal engine oil pressure. For a static axial face seal, pressure containment requires that the local O-ring contact pressure exceed the fluid pressure along the sealing line; however, a gross force comparison provides a useful upper bound on the separation tendency.

A conservative estimate of the pressurized area may be obtained by taking the area enclosed by the O-ring inner diameter. For a circular O-ring with center diameter $D_c = 50\text{ mm}$ and cross-section diameter $d = 4\text{ mm}$, the inner diameter is approximately

$$D_{\text{ID}} \approx D_c - d = 46\text{ mm}.$$

The corresponding pressurized area is

$$A_p \approx \frac{\pi}{4} D_{\text{ID}}^2 = \frac{\pi}{4} (46\text{ mm})^2 \approx 1.66 \times 10^{-3}\text{ m}^2.$$

For a representative hot-oil operating pressure in the range $\Delta p = 4 -- 6\text{ bar}$, the resulting hydraulic separation force is

$$F_p = \Delta p A_p \approx (0.4 -- 0.6) \times 10^6\text{ Pa} \times 1.66 \times 10^{-3}\text{ m}^2 \approx 660 -- 1000\text{ N}.$$

This force scale is comparable to, but generally lower than, the total stored compressive preload in the O-ring estimated above ($F_{\text{total}} \approx 0.55 -- 2.5\text{ kN}$ for 10--25% squeeze). More importantly, sealing is governed by *local contact pressure* rather than by net force balance. Typical O-ring contact stresses under nominal squeeze lie in the multi-megapascal range, whereas engine oil pressure remains well below 1 MPa. Consequently, under correct geometric support and load termination, the O-ring easily contains the applied oil pressure with substantial margin.

Further inspection identified radial interference between the oil filter canister and an overlong oil pan fastener located beneath the canister mouth. During installation, slight resistance was felt while tightening this fastener. This resistance was initially interpreted as normal thread engagement but is more consistently explained as the onset of lateral contact between the fastener tip and the thin-wall steel canister, introducing an unintended radial jacking load.

The mechanical response of the canister to this interference is documented in Fig. 2(a-c). After removal of the fastener, partial elastic spring-back was observed, but the canister did

not fully re-center on its own. Deliberate mechanical re-centering at the mouth was required to restore alignment, indicating that the dominant response was rigid-body motion rather than purely elastic deformation.

Because the canister passes through the proximal crankcase wall with radial clearance and is constrained only at a distal press-fit region, radial interference at the mouth produces local lateral displacement and slight angular rotation of the canister, effectively pivoting about the distal bore. This motion does not primarily unload the O-ring; instead, it compromises the axial backing normally provided to the thin metal shim at the canister mouth.

With axial support locally compromised, the O-ring continues to transmit its preload into the seal stack, as quantified above. Because the shim is no longer uniformly backed, this force is applied over a reduced and asymmetric area, causing the unsupported portion of the shim to plastically deform and translate axially. The resulting axial motion drives the elastomer laterally into the annular gap between the canister and the crankcase face, producing the observed external oil leak.

The leak therefore arises not from global loss of O-ring preload, but from a change in load path and local support conditions that allow a radially initiated disturbance to manifest as axial seal extrusion.

Distinguishing rigid-body motion from localized yielding is difficult *in situ*; however, both mechanisms are consistent with the observed seal extrusion shown in Fig. 1. The demonstrated ability to re-center the canister (Fig. 2) strongly supports a lightly retained, non-heroic press-fit rather than a rigidly fixed component.

5 Why This Failure Mode Is Subtle

This failure mode is particularly insidious because it combines multiple well-known Airhead narratives:

- Symptoms closely resemble common seal preload or elastomer creep issues.
- The engine continues to run normally.
- The initiating cause lies outside the expected seal load path, even though it is physically adjacent to the leak location.

In this case, the presence of a visibly damaged and displaced O-ring reinforced an incorrect initial diagnosis focused on elastomer behavior. Only after recognizing the canister displace-

ment and explicitly tracing axial load paths through the surrounding structure was the true cause identified.

Ironically, the resulting external oil leak served as a protective failure mode. Continued operation with a compromised seal may have prevented more serious internal bypass conditions by providing an early, visible indication of system distress.

Intentional Deviation from Field-Normal Repair

The immediate mechanical issue was resolved by re-centering the canister, a field-normal repair consistent with long-standing independent service practice. Nominal alignment was restored, and the system could have been reassembled and returned to service, as illustrated in Fig. 2. In many cases, this outcome would represent a reasonable and sufficient repair.

However, inspection revealed residual plastic deformation at the canister mouth. Although modest in magnitude, this deformation implied a permanent loss of roundness: once yielded, the mouth would no longer represent a pristine cylindrical reference. Any subsequent measurement of canister depth, shim stack height, or O-ring compression would therefore be referenced to a geometry that had already been compromised.

Because the canister mouth defines a precision sealing interface—one that must be evaluated by measurement rather than visual inspection—this residual deformation introduced an unacceptable degree of uncertainty. Even small geometric deviations could bias depth measurements, obscure loss of margin, or complicate future service decisions. For this reason, continued use of the deformed canister was judged to carry avoidable risk, despite the absence of immediate functional symptoms.

This assessment was reinforced by photographic documentation presented by Largiader, which illustrates the mechanically superior geometry of the later-style oil filter canister. The later design features a broader, flared, and axially flattened mouth that distributes contact pressure more uniformly and provides more stable backing for the O-ring and shim stack. In contrast, the earlier straight-cut geometry concentrates load at a relatively sharp edge, offering little tolerance once yielding initiates. In configurations where shims are not required, this sharp edge is inherently less stable: it promotes localized indentation, can abrade the O-ring under compression, and provides no geometric mechanism for re-centering or load redistribution.

Practical considerations also informed the decision. With the motorcycle already out of service during the winter season, the additional analysis and corrective effort imposed minimal

opportunity cost, allowing a more conservative, geometry-first approach without sacrificing riding time.

What initially presented as an assembly error was therefore reframed as an opportunity to replace a compromised component with a demonstrably better design. The analysis that follows reflects a deliberate choice to proceed beyond restored operability in order to establish a clean geometric baseline, quantify retention behavior, and replace service folklore with mechanically grounded understanding.

6 Canister Retention, Deformation, and Recovery

The oil filter canister is retained primarily by friction at a distal press-fit region within the crankcase bore. Under normal conditions, this retention interface experiences little direct loading from the sealing system, which reacts axial preload locally at the canister mouth. As a result, canister retention and seal integrity are governed by physically distinct mechanisms.

This section examines how unintended loading at the canister mouth affects retention behavior, deformation sequence, and recovery, without re-deriving the force transmission or geometric susceptibility established in Section 4.

6.1 Retention Characteristics of the Press-Fit Interface

The distal press-fit region provides radial constraint and modest axial retention through friction. It is not intended to react significant bending moments or lateral loads applied at the canister mouth. Consequently, when a radial or eccentric load is introduced near the mouth, the press-fit does not act as a rigid clamp.

Instead, the canister behaves as a lightly retained body with limited rotational stiffness, permitting small angular rotation and lateral displacement about the distal interface. This behavior is consistent with the observed ability to mechanically re-center the canister following load removal.

6.2 Deformation Sequence Under Unintended Loading

Eccentric contact at the canister mouth produces localized radial loading rather than uniform axial compression. Because the press-fit does not arrest this motion, the canister responds by pivoting slightly about the distal retention zone.

This motion alters local support conditions at the mouth without producing gross axial translation or loss of retention. The resulting deformation is therefore subtle: the canister remains seated and retained, while the geometry at the mouth is locally compromised.

6.3 Elastic Recovery and Permanent Set

Following removal of the unintended load, partial elastic recovery of the canister position was observed. However, full self-centering did not occur without deliberate mechanical intervention at the mouth.

This behavior indicates a combination of elastic rotation about the distal press-fit and localized permanent deformation at the mouth. The retention interface remains intact, but the canister no longer returns reliably to its original centered position on its own.

The observed recovery behavior supports the interpretation of the canister as a lightly retained component rather than a rigidly fixed one.

6.4 Retention Versus Seal Integrity

A critical outcome of this behavior is the decoupling of retention from seal integrity. The canister remains mechanically retained even as sealing margin is reduced or lost.

Because the press-fit interface remains engaged, there is no gross motion, noise, or immediate mechanical indication of distress. Seal degradation therefore progresses silently until extrusion or leakage becomes visible, as documented in Section 4.

This decoupling explains why normal engine operation can coexist with an active and progressively worsening sealing failure.

6.5 Diagnostic Implications

From a service perspective, retention alone is an unreliable indicator of system health. A canister that appears secure may nevertheless have experienced local displacement sufficient to compromise axial backing at the mouth.

Direct measurement of canister depth and careful inspection of sealing components are therefore essential diagnostic tools. Reliance on retention feel, torque feedback, or visual inspection alone is insufficient to detect this class of failure.

Understanding the retention behavior clarifies why the failure mode is latent and why its

cause is easily misattributed without explicit load-path analysis.

7 Canister Mouth Geometry and Contact Conditions

The oil filter canister is a thin-wall steel cylinder installed into a machined bore in the aluminum crankcase. Retention is provided by a distal press-fit region, while sealing is achieved locally at the canister mouth through axial compression of an elastomer O-ring. The geometric features of the canister mouth therefore govern how unintended external loads are introduced into the canister wall and how those loads are terminated.

This section focuses exclusively on the *geometric* aspects of the problem: mouth profile, local stiffness, contact susceptibility, and the constraints imposed by the surrounding structure. Force transmission, shim deformation, and sealing consequences are established separately in Section 3 and are referenced here only as needed.

7.1 Mouth Geometry Variants

Two canister mouth geometries are relevant to this investigation: an earlier straight-cut configuration and a later rolled-and-flattened configuration. While both provide an axial sealing land for the O-ring, their response to eccentric contact differs substantially.

In the straight-cut configuration, the canister wall terminates abruptly at a thin edge. The sealing land is narrow, and the local bending stiffness of the wall is low. This geometry offers minimal resistance to localized radial displacement when contact is applied near the mouth.

In contrast, the rolled-and-flattened configuration is formed by flaring the wall outward, rolling it inward, and flattening it axially. This process produces a thicker, work-hardened sealing land with increased local stiffness and a broader contact area. As a result, eccentric loads are distributed over a larger circumferential and axial region before being transmitted into the canister wall.

7.2 Geometric Susceptibility to Eccentric Contact

Although the oil pan fastener is nominally axial, its trajectory relative to the canister mouth is offset from the canister centerline. Any fastener protrusion beyond the intended design envelope therefore introduces the possibility of point or line contact at the canister mouth rather than uniform axial loading.

Such contact is inherently eccentric. The applied force is localized and acts at a radial offset, generating bending and lateral displacement rather than pure axial compression. The magnitude of the resulting displacement depends strongly on the mouth geometry and local stiffness, not on the strength of the distal press-fit region.

7.3 Constraint by the Distal Press-Fit

The canister passes through the proximal crankcase wall with radial clearance and is constrained only at a distal press-fit region. This constraint geometry permits small angular rotation and lateral motion of the canister when a radial load is applied at the mouth.

As a result, contact at the mouth does not primarily load the press-fit interface. Instead, the canister responds as a lightly constrained cantilever or pivoting body, with rotation occurring about the distal retention zone. This geometric arrangement explains why deformation and displacement localize at the mouth rather than along the cylindrical interface.

7.4 Geometric Consequences of Mouth Displacement

Once the canister mouth is displaced radially inward, axial backing conditions at the sealing interface are altered. The sealing stack remains nominally assembled, but local support is reduced or lost in the region of displacement. The mechanical consequences of this loss of backing, including load redistribution within the sealing stack and secondary shim deformation, are established quantitatively in Section 4.

From a geometric standpoint, the critical observation is that very small radial displacements at the mouth are sufficient to compromise local support conditions. Because sealing tolerances are tight, the geometry provides little margin for unintended contact without downstream effects.

7.5 Implications for Geometry-Controlled Failure Modes

The geometry of the canister mouth acts as both an initiator and a limiter of the observed failure mode. It defines where unintended contact can occur, how loads are introduced, and why deformation localizes at a single feature rather than being distributed throughout the structure.

These geometric characteristics explain why the failure mode is sensitive to configuration changes that appear benign at the component level. Once the mouth geometry permits

eccentric contact, subsequent mechanical effects follow directly from established load paths and material response, as developed elsewhere in this paper.

8 Fiche Interpretation and Configuration Anomaly

BMW parts fiches accurately specify component compatibility and fastener lengths for individual configurations. However, they do not encode three-dimensional interference constraints, nor do they account for cumulative configuration changes that arise across multiple service events. The anomaly examined here arises from this limitation rather than from incorrect parts selection.

This section addresses why the configuration remained fiche-compliant while still permitting an unsafe interaction with the oil filter canister.

8.1 Nominal Fastener Specification

In the stock configuration, the oil pan fastener located beneath the oil filter canister mouth is intentionally short. This ensures that the fastener cannot intrude into the filter cavity or contact the canister, even in the presence of manufacturing tolerances or service variation.

When optional components such as distance rings or skid plates are added, the fiche correctly specifies longer fasteners to accommodate the increased stack height. In isolation, these substitutions satisfy thread engagement and clamp load requirements.

8.2 Implicit Assumptions in Fiche-Based Validation

Fiche compliance implicitly assumes that substituted fasteners preserve all original clearance relationships. This assumption holds only if the added components do not alter fastener trajectory relative to sensitive internal features and if no fastener extends beyond the original design envelope.

In the present case, these assumptions were violated subtly. The longer fastener remained acceptable by fiche criteria but extended sufficiently to approach the canister mouth under certain conditions. The fiche does not—and cannot—encode this spatial relationship.

8.3 Why the Anomaly Is Difficult to Detect

The configuration produces no obvious interference at rest. Fastener installation torque feels normal, and visual inspection does not reveal contact without disassembly. Moreover, as shown in Section 3, the critical mechanical consequences arise during fastener removal rather than during installation.

This temporal separation between cause and effect further obscures the role of the fastener and delays correct diagnosis. Even after a sealing failure is observed, attention is naturally drawn to the O-ring rather than to adjacent hardware that appears fiche-compliant.

8.4 Limits of Documentation-Based Safeguards

This case highlights a fundamental limitation of documentation-based safeguards: they enumerate allowable parts, not allowable interactions. When configurations evolve incrementally, especially across independent service actions, spatial interference conditions can emerge without any single step violating documentation guidance.

Avoiding this class of failure therefore requires either explicit clearance verification during service or conservative fastener selection that preserves original intrusion margins, independent of fiche minimums.

8.5 Generalization Beyond the Present Case

The issue described here is not unique to the oil filter canister. Any system that combines optional hardware, fastener length substitution, and sensitive internal features is susceptible to similar latent interference modes.

Fiche compliance should therefore be regarded as a necessary but insufficient condition for mechanical safety in modified or evolved assemblies.

9 Canister Depth Control Strategy (Largiader-Aligned)

Given the sensitivity of the seal stack to axial placement, the most robust depth-control strategy is to reference the *installed depth of the original canister*, rather than relying on nominal drawing values or assumed axial stops. Because the original and replacement canisters share the same overall length and geometry, effective depth control is achieved by

controlled installation relative to the original seating condition.

Any residual variation can then be accommodated at the canister mouth using standard external shims, which remain directly observable and adjustable during assembly. A critical constraint is the avoidance of a *proud* canister condition, which could introduce unintended axial contact or preload at the bore end and compromise seal behavior. Accordingly, depth control should be achieved through measurement, seating discipline, and external shimming alone.

Background observations. Independent service experience, including long-running shops such as **Duncan's Beemers**, has repeatedly highlighted oil filter canister depth as a non-trivial variable influenced by crankcase machining tolerance, service history, and seating behavior. This reinforces the need for explicit depth measurement and control rather than reliance on nominal dimensions or assumed axial stops.

9.1 Percent O-Ring Compression as a Secondary Check

In addition to groove-depth and stack-height methods, some practitioners evaluate the oil filter seal using a percent O-ring compression metric. This approach is commonly presented in instructional material from Brooks & Brandon's *Airhead Garage* and appears in various community references.

The compression percentage is computed as

$$\% \text{ compression} = \frac{O + nS - C - D}{O} \times 100\%, \quad (1)$$

where:

- O is the O-ring cross-section thickness (nominally ~ 4.0 mm for the white O-ring),
- n is the number of shims,
- S is the thickness of each shim (nominally 0.3 mm),
- C is the oil filter cover gasket thickness (typically $C = 0$ in modern practice, as the gasket is often omitted),
- D is the measured canister depth from the crankcase face.

A commonly recommended acceptance band is 10–25% compression, which corresponds to approximately 0.4—1.0 mm of O-ring squeeze when $O = 4.0$ mm. This range overlaps with, and is broadly consistent with, the groove-depth guidance documented by Largiader.

Percent O-ring compression is included here only as a secondary consistency check. By construction, it cannot detect loss of axial backing caused by radial canister displacement, since such displacement alters load paths without necessarily changing the nominal compression value. In the present case—precipitated by an unforced assembly error upstream of the sealing interface—numerically acceptable compression would have been computed even though the sealing geometry had already been compromised. This limitation does not diminish the utility of the method under normal conditions, but it underscores that compression checks assume intact canister geometry and are not diagnostic of upstream mechanical interference.

10 Removal and Installation Tooling: Practical Reality

Oil filter canister service requires controlled axial force applied through positive mechanical engagement while maintaining alignment in a deep, blind bore. Friction-only methods are unreliable and risk secondary deformation or bore damage.

Observed canister mobility indicates that the required axial forces are moderate in magnitude; however, successful extraction depends far more on *alignment control and tactile feedback* than on raw force capability.

10.1 Field-Expedient Extraction Method (As Executed)

In principle, a purpose-designed internal puller that positively engages a distal shoulder would be an attractive solution. In practice, the as-installed canister and all observed replacement canisters lacked robust distal cut-outs, shoulders, or undercuts suitable for conventional internal-jaw pullers. While a distal screw-based puller could be imagined, it would require an extremely shallow, sharp engagement lip and precise geometry; it is not clear that such a tool is feasible or that one exists. No commercially available or commonly cited example is known to the author.

Given these constraints, extraction in this case was performed using a controlled drive-out method enabled by a single radial hole in the canister wall.

Concept. A radial hole is drilled through the thin canister wall at an accessible location. A steel screw (or closely fitting pin) is inserted through the hole to act as a temporary drive feature. Axial extraction force is then applied by tapping on this feature *while simultaneously applying counter-torque and alignment control at the canister mouth*. These actions are not sequential; they occur continuously and in concert.

Important safety note. This method carries inherent risk and should not be treated as a generic procedure. Specific hazards include: (i) generation of metal chips near the oil system, (ii) risk of drilling into the aluminum crankcase if depth control is lost, and (iii) risk of cocking the canister and damaging the bore. Execution relies heavily on operator judgment, tactile sensitivity, and continuous control rather than prescriptive steps.

Procedure outline (conceptual, high level).

1. **Access and preparation.** Remove components as needed to obtain clear access to the canister and lower cavity. Clean the work area and establish chip-capture measures (grease, rags, shielding, suction, and post-operation flushing).
2. **Hole placement and drilling.** Select a location clearly within the thin-wall region of the canister (not through the rolled mouth). Drill only through the canister wall, using positive depth control. The intent is to create a controlled drive feature, not a structural modification.
3. **Simultaneous extraction and alignment control.** Insert a steel screw or pin through the hole. Apply light tapping force to the drive feature while *simultaneously* applying reactive counter-torque at the canister mouth using a lever (e.g., a tire iron). The operator can feel the upward axial reaction moment transmitted through the counter-torque tool. Tapping, alignment correction, and axial guidance occur continuously and together, not as discrete steps.
4. **Continuous tactile monitoring.** The canister's motion, resistance, and tendency to tilt are assessed continuously through feel. Any increase in side resistance or loss of smooth axial motion requires immediate corrective action. The objective is to maintain predominantly axial translation throughout the process.
5. **Completion and inspection.** Once released, remove the canister by hand. Carefully remove all chip containment measures and clean the cavity thoroughly. Inspect the bore for scoring, raised material, or damage before proceeding with installation.

Rationale. The primary risk in a drive-out method is bore damage caused by a cocked canister. Successful execution depends on continuous, reactive alignment control informed by tactile feedback rather than on incremental or scripted actions. The observed non-heroic retention fit (Section 6) makes this approach feasible, but only when handled with appropriate sensitivity and restraint.

Status and documentation. Figures 3a–3c document the executed extraction, including localized deformation at the drive-hole site, simultaneous application of counter-torque during tapping, and final removal. The removed canister was rendered unsuitable for reuse, but inspection confirmed that extraction forces were localized and that the crankcase bore was not subjected to damaging side loads.

11 Installation Execution and Observed Behavior

Installation of the replacement oil filter canister was performed in a single, deliberate operation following removal of the deformed original sleeve and inspection of the crankcase bore. The objective was to restore a clean geometric baseline while enforcing a controlled axial load path and avoiding secondary damage to the crankcase.

Prior to insertion, the distal end of the replacement canister was cleaned with gray Scotch-Brite to remove light surface oxidation and condition the surface for uniform contact during seating. The contact region was then lightly lubricated with engine oil to reduce insertion friction and mitigate the risk of galling.

As received, the replacement canister also carried an adhesive-backed BMW identification label on the outer surface. While appropriate for parts handling and inventory control, the label and its adhesive residue are incompatible with controlled press-fit installation. Complete removal proved nontrivial, requiring multiple applications of a citrus-based solvent (Goo-Gone) and careful scraping with a plastic blade to avoid surface damage. Final cleaning ensured a uniform metal-to-metal contact condition prior to insertion.

To further reduce required driving force, moderate external heat was applied to the surrounding crankcase using a heat gun (Fig. 3e). Heating was limited to raising the case to warm-to-touch temperature. The intent was to take advantage of differential thermal expansion between the aluminum crankcase and the steel canister, not to soften materials or alter interference characteristics. Lower ambient temperature further increased the available thermal expansion differential.

Axial insertion force was applied using a temporary driver assembled from existing BMW Airhead engine service tools (Fig. 3f). Although not a dedicated single-purpose driver, the stacked-tool arrangement was selected specifically to enforce a purely axial load path and to bear against the reinforced mouth region of the canister rather than the thin wall. This configuration provided adequate concentric guidance and allowed controlled tapping without introducing bending moments or off-axis loading.

The canister advanced smoothly with modest applied force, consistent with the light-retention behavior inferred from earlier observations. No abrupt resistance, stick-slip motion, or asymmetric engagement were encountered during insertion.

The decision to replace the canister rather than attempt re-centering was based on the mechanical advantages of the later rolled-and-flattened mouth geometry, which are developed in detail in Section 7.1. In the context of this repair, replacement ensured restoration of both geometric stiffness and sealing margin, rather than relying on partial recovery of a locally compromised feature.

Insertion was halted at the previously marked reference line corresponding to the installed depth of the original canister (Fig. 3g). Final position was at, or marginally beyond, this reference, reflecting a conservative approach to depth control pending final measurement. Visual inspection into the installed canister (Fig. 3h) confirmed improved concentricity and uniform seating relative to the removed component.

At no point during the installation was corrective re-centering required, and no evidence of asymmetric resistance or elastic spring-back was observed after seating. These observations are consistent with a clean, undistorted bore and with the mechanically more forgiving mouth geometry of the later-style canister.

For completeness and future serviceability, a conceptual dedicated installation driver is described elsewhere in this work. While such a tool was not fabricated for this installation, the stacked factory-tool arrangement employed here satisfied the same functional requirements: axial load application, concentric engagement, and avoidance of thin-wall contact.

12 Execution Summary and As-Built Measurements

At the conclusion of this work:

- Two replacement oil filter canisters were received and verified to be visually consistent with BMW part 11 11 1 338 203.

- The original canister was successfully removed using a field-expedient drive-out method, and the crankcase bore was subsequently inspected and cleaned.
- Although a dedicated canister installation driver could be designed in accordance with Table 1, the present installation was performed using a combination of BMW engine tools that satisfied the same functional requirements.
- Final depth control was achieved through direct measurement by transferring the wear mark from the original canister onto the replacement canister (Fig. 3d), and tapping the replacement canister into the bore until this reference mark was reached (Fig. 3g). This approach leverages the confirmed axial equivalence of the original and replacement canisters, with any residual variation accommodated using external shims.

Table 1: Suggested installation driver dimensions (later-style canister).

| Feature | Suggested value | Notes |
|-------------------------|--------------------------------|---------------------------------------|
| Material | 6061-T6 aluminum or mild steel | Aluminum preferred (gentler contact) |
| Overall length | 100 — 130 mm | Long enough to tap comfortably |
| Body diameter | 45 — 55 mm | Stable striking surface |
| Pilot (recess) diameter | 47.5 mm | Clearance fit inside nominal 48 mm ID |
| Pilot depth | 4 — 6 mm | Enough to self-center |
| Annular bearing face OD | 52 mm (max) | Must clear case opening |
| Annular bearing face ID | 47.5 mm | Matches pilot diameter |
| Edge breaks | 0.5 mm chamfer | Prevent gouging |
| Strike face | Flat and square | Optional slight crown acceptable |

12.1 Measured Dimensions and Implications

Post-removal and post-installation measurements provide additional context for both the failure mechanism and the corrective strategy:

- The axial wear band on the original canister was measured at 11.59 mm from the mouth.
- Two independent measurements of the crankcase bore depth yielded 11.87 mm and 11.91 mm, confirming that seating to the original wear line retained margin to the bore floor.

- The removed canister measured approximately 137.87 mm in overall length.
- The replacement canister measured approximately 137.63 mm in overall length.

The small apparent difference in measured canister length is attributed to normal manufacturing tolerance and measurement uncertainty rather than to a designed or functional length change. For purposes of installation and depth control, the canisters are treated as equivalent in effective axial length.

Following installation, the canister depth measured an average of 3.90 mm from the crankcase face using a micrometer depth gauge, compared to a pre-removal value of approximately 3.60 mm. The increase in installed depth is attributed to unavoidable bore working during the interference event, extraction, and subsequent re-centering process. Depth measurements were repeated at multiple circumferential locations to confirm consistency and repeatability.

For a confirmed depth near 3.8 mm–3.9 mm, both the groove-depth relationship derived by Brooks and Brandon (*Airhead Garage*) and the tabulated shim guidance presented by Largiader indicate that a two-shim stack is appropriate. This configuration achieves the desired O-ring compression while preserving external observability and adjustment capability at the canister mouth.

13 Lessons Learned

This investigation highlights several lessons that extend beyond the specific oil filter canister configuration examined here. Each lesson emerges from the interaction between geometry, load path, and service practice rather than from a single isolated error.

13.1 Geometry Governs Latent Failure Modes

The failure mechanism did not arise from inadequate material strength or insufficient sealing capacity. Instead, it was governed by a geometric vulnerability at a thin, locally compliant feature. Once unintended contact altered support conditions at the canister mouth, subsequent mechanical consequences followed directly.

This emphasizes that latent failures are often geometry-controlled rather than strength-controlled, particularly in thin-walled or tolerance-sensitive systems.

13.2 Nominally Axial Actions Can Produce Off-Axis Effects

Although fasteners are commonly treated as purely axial load paths, this case demonstrates that trajectory, clearance, and transient contact conditions can convert nominally axial actions into eccentric loading. Critical effects may occur during installation or removal rather than during steady-state operation.

Service procedures must therefore consider intermediate and transient conditions, not just final assembled states.

13.3 Retention and Sealing Are Distinct Failure Domains

The canister remained mechanically retained while seal integrity was quietly compromised. This decoupling allowed the failure to remain latent until leakage occurred.

Systems in which retention and sealing functions are physically separated should be evaluated explicitly for failure modes that degrade one function without immediately affecting the other.

13.4 Documentation Ensures Compatibility, Not Interaction Safety

Parts documentation correctly specified compatible components but did not prevent an unsafe interaction from emerging as the configuration evolved. Documentation enumerates allowable parts; it does not encode three-dimensional interference constraints.

When optional hardware and fastener substitutions accumulate over time, clearance verification must supplement documentation-based validation.

13.5 Measurement Outperforms Visual Inspection

The deformation responsible for seal failure was subtle and not readily apparent through visual inspection alone. Measurement of canister depth and inspection of sealing stack behavior were essential to correct diagnosis.

Where tolerances are tight and consequences are high, quantitative measurement should be favored over qualitative assessment.

14 Conclusion

This study demonstrates how a configuration that is locally compliant with parts documentation can nevertheless produce a latent failure mode through unintended geometric interaction. The observed oil leak did not result from improper assembly, insufficient sealing capacity, or material deficiency, but from a change in load path initiated by an unexpected contact condition.

By separating observation, force-scale analysis, geometry, retention behavior, and documentation limits into distinct sections, the underlying mechanism becomes clear. A localized disturbance at the canister mouth altered support conditions within the sealing stack, allowing normal preload and operating pressures to produce progressive extrusion and leakage without loss of overall retention.

The broader implication is not limited to BMW Airhead engines. Any system combining thin-walled features, tight sealing tolerances, optional hardware, and evolving service configurations is susceptible to similar failure modes. As systems age and modifications accumulate, interaction effects increasingly dominate over component-level considerations.

Avoiding this class of failure requires attention to geometry, load introduction, and transient service conditions, rather than reliance on documentation or nominal design intent alone. When these factors are explicitly considered, latent failures can be identified and mitigated before manifesting as operational faults.



Figure 1: O-ring and shim condition as found. The shim shows smooth, continuous plastic curvature in the region rendered unsupported by radial displacement of the canister mouth. The O-ring appears nominal in the images and is included for reference; its contribution to the observed deformation arises from load redistribution under geometric constraint rather than from visible material distortion.

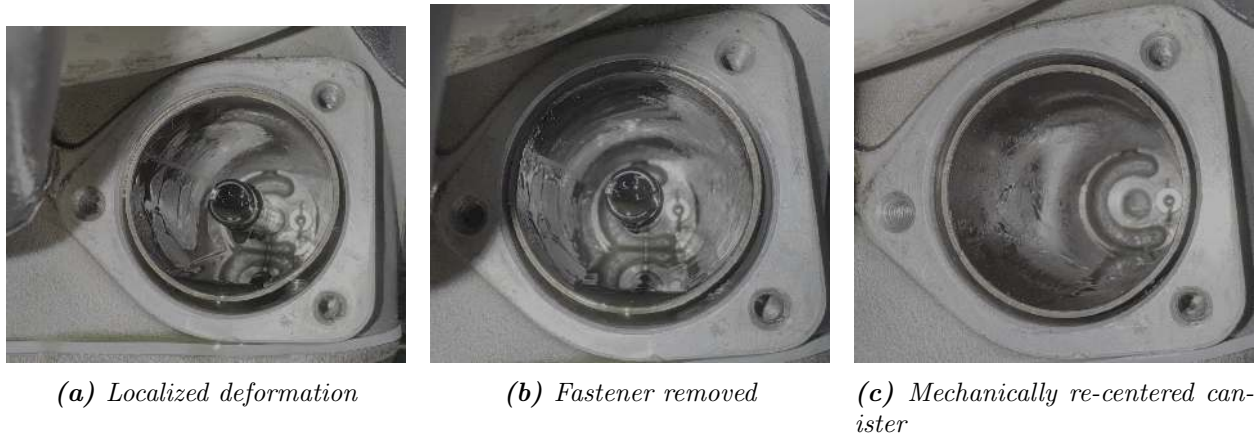


Figure 2: Canister displacement and recovery sequence, demonstrating dominant rigid-body motion about the distal press-fit region. (a) Localized deformation at the canister mouth caused by unintended radial jacking. Note the bolt protrusion visible in the lower-right quadrant (near the 5 o'clock position). (b) After fastener removal, partial elastic spring-back occurs, but full self-centering does not occur without an applied corrective moment. (c) Deliberate mechanical re-centering at the mouth restores nominal alignment. The central PIPE was removed at this stage to provide clearance for controlled levering without interference.



(a) Localized wall deformation during drive-out tapping. The bolt orientation was perpendicular to the canister prior to tapping. Plastic deformation and bolt rotation within the thin sheet are unavoidable.



(b) Counter-torque applied to maintain axial alignment and prevent bore damage.



(c) Canister removed after controlled tapping sequence.



(d) Replacement canister distal end cleaned and lightly oiled prior to insertion. Note the traced insertion depth check line.

Figure 3: Extraction and installation sequence (1 of 2).



(e) Crankcase warmed with heat gun to reduce insertion force via differential expansion.



(f) Temporary axial driver assembled from available engine tools.



(g) Final installed position relative to the reference depth mark.



(h) View into installed canister showing improved concentricity and self-centering.

Figure 3: Extraction and installation sequence (2 of 2).